Chapter 2
Identifying Hidden Resources in Solar Home Systems as the Basis for Bottom-Up Grids

Hannes Kirchhoff

Abstract In the context of the modern energy access challenge, one new pathway towards electrification is to make use of hidden resources already in the field through small microgrids. In particular, this paper analyses the amount of excess energy of medium sized (65 Wp) solar home system (SHS) located in Bangladesh. The SHS is modeled using synthetic load curves and a sophisticated battery model that accounts for battery ageing. The simulation shows that more than 30 % of the electricity potentially generated by the SHS remains unused.

Keywords SHS · Hidden resources · Microgrid · Bottom-up

Introduction

The energy access challenge presents itself on several fronts at the same time. While there are still more than 2.3 billion people without reliable access to electricity (United Nations Foundation 2012), a carbon lock-in is on the horizon if the power sector does not turn green quickly (IEA 2011, p. 3). For individuals who currently do not have access to modern energy services that are "affordable, clean, reliable, and safe" (Legros et al. 2009, p. 3) this translates into high prices and uncertain timelines for access.

As pointed out by Tenenbaum et al. (2014), it is time for the "second", decentralized track in electrification. A track that does not rely on central entities but can grow from the bottom-up. The "swarm electrification" approach (Groh et al. 2013), shows a pathway for how this can be done, building on the existing infrastructure, such as the 2.6 million solar home systems (SHS) already installed in Bangladesh (IDCOL 2013). SHS are linked to form small microgrid clusters that can gradually be extended by going through different stages, c.f. Fig. 2.1. The process is a step by

H. Kirchhoff (✉)
Microenergy Research Group, TU Berlin, Hardenbergstraße 16-18, 10623 Berlin, Germany
e-mail: hannes.kirchhoff@microenergy-systems.de

S. Groh et al. (eds.), *Decentralized Solutions for Developing Economies*,
Springer Proceedings in Energy, DOI 10.1007/978-3-319-15964-5_2

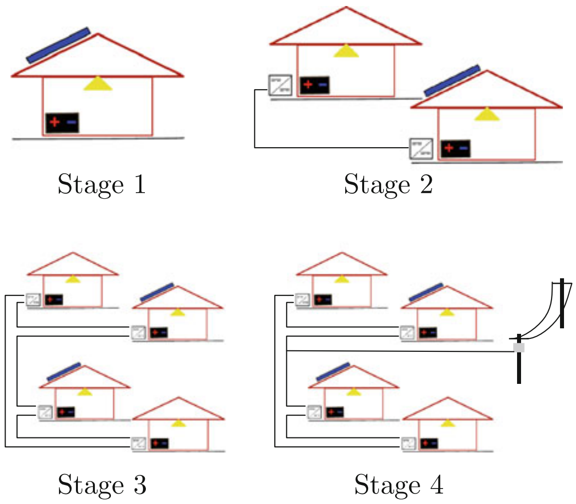

Fig. 2.1 Step by step bottom-up electrification

step bottom-up approach that eventually leads to coverage of a whole village. The formed microgrid can, if desired, even be connected to the main grid. There is limited literature available on interconnected SHS, however, one simulation showed a 15 % saving in generation capacity required when eight large SHS located in Tanzania were connected (Unger and Kazerani 2012).

Research Objectives

This paper addresses the perspective for a single SHS in the initial process of swam electrification, showing the potential for energy sharing. Hence, the hidden resources in terms of excess energy that remains unutilized in normal SHS operation is investigated on.

Methods

The 65 W_p SHS package under the IDCOL solar program is simulated for the course of one year using Matlab Simulink with 5 min intervals. The SHS package consists of a 65 W_p solar panel and a 100 Ah battery. Details of the respective component modeling are as follows.

Table 2.1 Parameters used in the PV module model

Parameter at standard test conditions, from Kyocera (2007)	Value
V_{MPP}	17.4 V
I_{MPP}	3.75 A
V_{OC}	21.7 V
I_{SC}	3.99 A
K_v	−0.0821 V/K
K_i	0.00159 A/K
Parameters obtained using Villalva et al. (2009)	**Value**
a	1.3 [–]
N_s	36 [–]
R_p	266,565 Ω
R_s	0.2454 Ω

Solar Module Simulation

For the model in this paper, the SHS is equipped with a 65 W_p multicrystal PV module, fitted to data sheets from Kyocera KC65T panel (Kyocera 2007), which is modeled using a mathematical model developed by Villalva et al. (2009). This model is an improvement of the single diode equivalent circuit and can be easily adapted to different panels. The work presented in the paper includes an algorithm to determine the best fitting parameters for the shunt resistance R_S and the parallel resistance R_P requiring only datasets at open and short circuit as well as at the maximum power point (MPP). These parameters are then used to model the characteristic current behavior as in (2.1) where V_t is the thermal voltage and a the ideality factor of the diode. The parameters used are listed in Table 2.1.

$$I_{PV} = I_0 \cdot \left[\exp\left(\frac{V + R_S \cdot I}{V_t \cdot a}\right) - 1\right] \tag{2.1}$$

The temperature influence on the panel are reflected on through the temperature coefficient for voltage K_V and the temperature coefficient for current K_I.

The model is verified with the electrical performance at nominal operating cell temperature which is given in the datasheet (Kyocera 2007), producing an error of less than 0.4 %.[1]

The influence of ambient temperature is most critical for the simulation of the PV panel where energy output is decreased for higher temperatures. Hence, a conservative assumption with a constant ambient temperature of 30 °C is taken. The temperature of the cells is modeled as being directly proportional to the irradiation G, as in (2.2). This approach is proposed by Hansen et al. (2000, p. 14).

[1] Input values are G = 800 W/m², T_{cell} = 47 °C and V_{PV} = 15.3 V. The datasheet states 46 W output and the model calculates 46.15 W.

$$T_C = T_A + 0.03\frac{\mathrm{C}\cdot\mathrm{m}^2}{\mathrm{W}}\cdot\mathrm{G} \tag{2.2}$$

Real solar data for Dhaka of the year 2001 is used, specifically global horizontal solar insulation data from NREL (2005). The panel's orientation is assumed as perfect south and 24° tilt to allow for maximum generation. Correction factors for this tilt are based on data from Boxwell (2013).

Battery Model

The battery modeling has to cover a wide range of parameters and constants, but there are essentially only two variable inputs into the model during the simulation: temperature and current. Corresponding to the ambient temperature, the battery temperature is assumed constant at 30 °C. This assumption is based on the fact that the current flows to and from the battery are relatively small and combined with the large surface to volume ratio of the battery should not lead to mayor warming effects (Boldt 2012).

Thus, the only remaining input variable is the current. The output parameters are the terminal voltage of the battery the state of charge (SOC) and, as a lifetime monitoring variable, the remaining capacity of the battery. Degradation and corrosion lead to reduction in capacity, which is reflected in the state of health (SOH). For batteries in electric vehicles the SOH is often defined so that it reaches zero when the remaining capacity is 80 % (Lam 2011). This does not necessarily hold true for batteries in SHS as the reduced capacity can still be used. Hence, in this paper the definition as in (2.3) is utilized, details on the calculation of the remaining discharge capacity $C_d(t)$ are given in Bindner et al. (2005) and Boldt (2012).

$$SOH = \frac{C_d(t)}{C_d(t=0)} \tag{2.3}$$

The terminal voltage U_{bat} is obtained by multiplying the cell voltage U_{cell} by the number of cells (six). The cell voltage is derived by using a set of two Shepherd Equations, one for charging (2.4) and one for discharging (2.5), where the SOC and DOD are the state of charge and depth of discharge respectively.

For I > 0:

$$U_{cell}(t,I) = U_0 - g\cdot DOD + \rho_c(t)\cdot\frac{I(t)}{C_N} + \rho_c(t)\cdot M_c\cdot\frac{I(t)}{C_N}\cdot\frac{SOC(t)}{C_c - SOC(t)} \tag{2.4}$$

For I ≤ 0:

$$U_{cell}(t,I) = U_0 - g\cdot DOD + \rho_d(t)\cdot\frac{I(t)}{C_N} + \rho_d(t)\cdot M_d\cdot\frac{I(t)}{C_N}\cdot\frac{DOD(t)}{C_d(t) - DOD(t)} \tag{2.5}$$

The Eqs. (2.4) and (2.5) can be both be rearranged so that each constitutes of one portion independent of the battery current and the other part dependent on the battery current. These are the values used for a simple equivalent circuit of the battery in the SHS model with a controlled voltage source (U_0) and an internal resistance (R_i) in series. Ageing effects are reflected in the model that are related to the following stress factors:

- *Time between full charges*, in particular modeling the build- up of irreversible sulphation,
- *Partial cycling* by taking into account the end of charge voltage when crossing over a SOC value of 90 % but not reaching 100 % which is critical for corrosion,
- *Ah-throughput* by evaluating the total discharge current in a weighted number of cycles which is an indication for the loss of active material as well as increased stratification,
- *Low discharge rates* which enhance stratification,
- *High temperature* is reflected in all relevant factors, in particular the build-up of the corrosion layer and the effect of gassing.

Charge Controller

The charge controller was modeled with an overcharge and a deep discharge protection. The threshold values for theses operations were taken from the IDCOL SHS program specifications and translated from voltage cut-off values to SOC-values. As shown in Fig. 2.2, the deep-discharge protection is activated after crossing 30 % SOC and the load is reconnected at 50 % SOC. Once the battery is

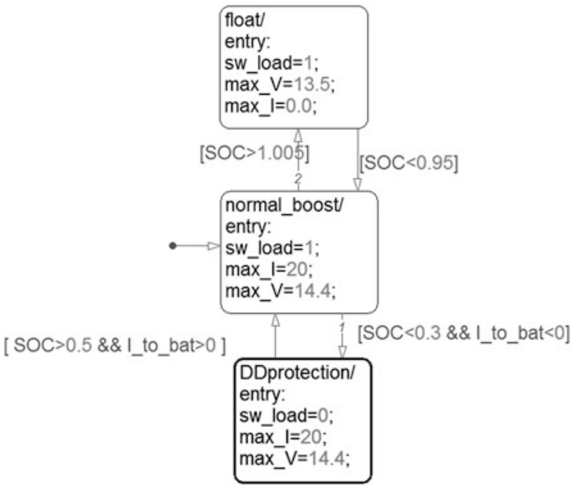

Fig. 2.2 Model for the charge controller

fully charged, the charge controller changes the charging mode from boost to float, limiting the charging voltage to 13.5 V.

Load Profile

As no real data on the usage pattern was available, literature values are used and combined to form a synthetic load curve. According to UNFCCC (2012, p. 6), 65 W_p SHS in Bangladesh are typically equipped with loads given in Table 2.2. A aggregate load of 43 W is used between 3 and 4 h per day, resulting in a daily energy consumption of 162 Wh.

However, other authors have argued that demand can be higher due to daily operation of up to 5 h per day (Khadem 2006, p. 4). To account for this discussion, an extensive use case of 240 Wh/d with longer usage hours and additional devices is also considered (c.f. Table 2.3). It is assumed that this extensive use case is applicable once in a week. This is simulated by giving a 6/7 probability to a 162 Wh load day and a 1/7 probability to a 240 Wh load day. User behavior, such as decreased demand when charge controller indicates a low SOC is not taken into account. The load distribution over the day is taken from Khadem (2006, p. 4).

In addition to the above, a daily noise level of 15 % and an hourly noise level of 20 % is added as suggested by Hafez and Bhattacharya (2012, p. 8), as shown in the exemplary profile in Fig. 2.3.

In the simulation, loads are modeled as a variable resistor. The value of the resistor is calculated by taking an average battery voltage of 13 V into account.

Table 2.2 Loads for normal use day (UNFCCC 2012, p. 6)

Appliance	Load (W)	Usage (h/d)	Daily demand (wh/d)
5 CFL lights	30	4	120
Black and white TV	10	3	30
Mobile charger	3	4	12
Total			162

Table 2.3 Loads for an extensive use day

Appliance	Load (w)	Usage (h/d)	Daily demand (wh/d)
5 CFL lights	30	5	150
Black and white TV	10	5	60
Radio/cassette player	5	2	10
Mobile charger	2 × 3	5	30
Total			240

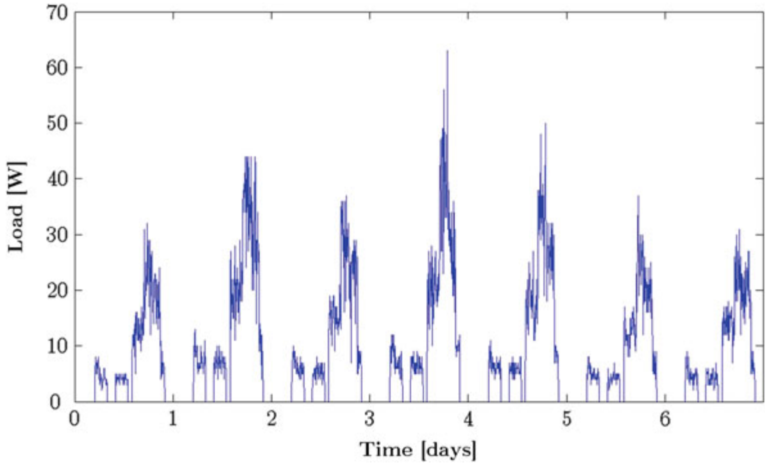

Fig. 2.3 Exemplary weekly load profile for one SHS

Results

For the simulated SHS located in Bangladesh, generation significantly exceeds the demand. Figure 2.4 shows how the daily generated energy is much larger than the daily demand for large parts of the year. Only in the beginning of the second half of the year does the daily demand occasionally exceed the daily generation.

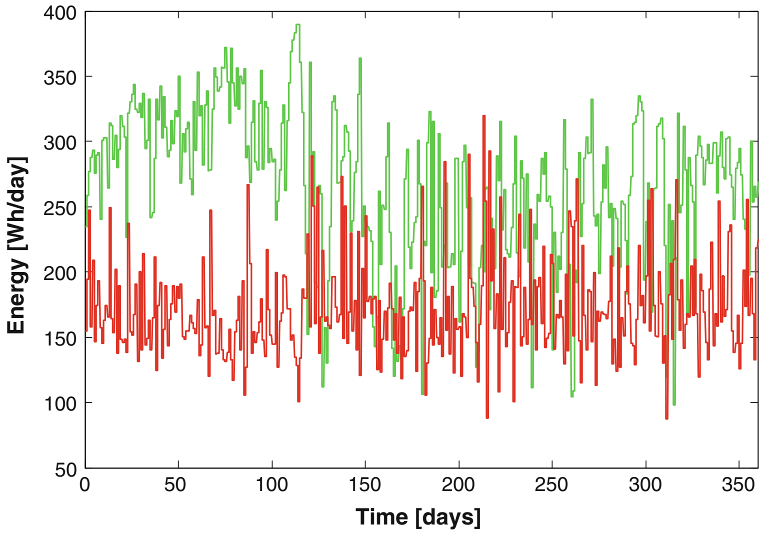

Fig. 2.4 Daily generation (*green*) and demand (*red*)

Table 2.4 Simulation results

Parameter	Value	Unit
Total potential generation	97.5	(kWh)
Total excess generation	31.1	(kWh)
Ratio excess generation	31.9	(%)
Total demand	62.0	(kWh)
Total disconnected load	0.0	(kWh)

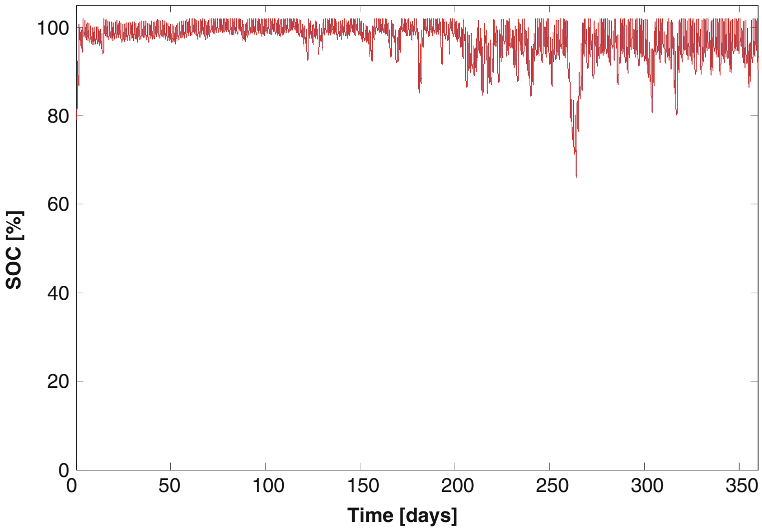

Fig. 2.5 SOC over the course of a year

Over the course of a year a total potential energy generation of 97.5 kWh was obtained, of which 31.9 % was not harvested and hence not utilized. The total demand of 62.0 kWh was completely supplied for, as given in Table 2.4.

The state of health (SOH) of the battery, defined as the ratio of the remaining capacity over the initial capacity, is at 96.8 % at the end of one year. The loss of capacity amounts to 2.5 % due to corrosion and 0.7 % due to degradation. The reason for this healthy operation is indicated in the SOC curve, as given in Fig. 2.5. The battery hardly goes into low SOC values in normal operation. The SOC falls under 80 % on only one occasion during the second half of the year.

Discussion

The results of this paper show a strong potential for interlinking SHS with other units. More than 30 % of the energy generated was dumped. However, there are a number of losses that have not been accounted for including reflection, dirt, shading or losses in the domestic wiring which could influence the outcome of this value. The assumptions made for the load profile play a critical role. In particular, seasonal load variation is not being accounted for which could have a large impact.

Nonetheless, there is a significant amount of energy hidden and available to be sold from the SHS owner to a small microgrid cluster. The initial connection to another household with a small battery that can store and use this energy and thus does not require any separate generation capacity could be the starting point for such a bottom-up electrification scheme.

Acknowledgments The author would like to thank the *Gesellschaft von Freunden der TU Berlin e.V.* for their support and the opportunity to present this work at the *MES-BREG 2014 Symposium: Innovating Access for Remote Areas | Discovering Untapped Resources* in Berkeley.

References

Bindner, H., Cronin, T., & Lundsager, P. (2005). *Lifetime modelling of lead acid batteries*. Roskilde: Risø National Lab, Wind Energy Department.

Boldt, F. (2012, March 8). *Simulation of micro electricity systems for on and off grid applications-focusing on the analysis of battery ageing and design of a system controller* (M.S. thesis, Dept. Eng.). Berlin: Hochschule für Technik und Wirtschaft Berlin.

Boxwell, M. (2013). Dhaka average solar insolation. Retrieved August 27, 2013, from http://solarelectricityhandbook.com/solar-irradiance.html.

Groh, S., Philipp, D., Lasch, B. E., & Kirchhoff, H. (2013). Swarm electrification—suggesting a paradigm change through building microgrids bottom-up. In *Energy systems in transition: Inter- and transdisciplinary contributions* (pp. 212–217). Karlsruhe: Helmholtz Association.

Hafez, O., & Bhattacharya, K. (2012). Optimal planning and design of a renewable energy based supply system. *Renewable Energy*, *45*, 7–15. Retrieved from http://www.scribd.com/doc/121420013/Optimal-planning-and-design-of-a-renewable-energy-based-supply-system-for-microgrids.

Hansen, A., Sørensen, P., Hansen, L., & Bindner, H. (2000). *Models for a stand-alone PV system*. Risø: Risø National Laboratory.

IDCOL. (2013, November). Renewable energy projects—IDCOL solar energy program. Retrieved January 30, 2014, from http://www.idcol.org/energyProject.php.

IEA. (2011). *World energy outlook 2011—executive summary*. Paris: International Energy Agency.

Khadem, S. K. (2006). *Feasibility study of wind home system in coastal region of Bangladesh*. Colorado: Homer Energy.

Kyocera. (2007). *KC65T—high efficiency multicrystal photovoltaic module* (Datasheet). Retrieved from http://www.kyocerasolar.com/assets/001/5170.pdf.

Lam, L. (2011, August 23). *A practical circuit-based model for the state of health estimation of Li-ion battery cells in electric vehicles* (M.S. thesis). Delft: University of Technology Delft, Department of Electrical Sustainable Energy.

Legros, G., Haver, I., Bruce, N., & Bonjour, S. (2009). *The energy access situation in developing countries: A review focusing on the least developed countries and Sub-Saharan Africa*. New York: United Nations Development Programme and World Health Organisation.

NREL. (2005, March 5). Solar: hourly solar (direct normal (DNI), global horizontal (GHI), and diffuse) data for select Bangladesh stations from NREL.

Tenenbaum, B. W., Greacen, C., Siyambalapitiya, T., & Candelaria, J. (2014). *From the bottom up: How small power producers and mini-grids can deliver electrification and renewable energy in Africa*. Washington, DC: The World Bank.

UNFCCC. (2012, May 29). Installation of solar home systems in Bangladesh. UNFCCC.

Unger, K., & Kazerani, M. (2012). Organically grown microgrids: Development of a solar neighborhood microgrid concept for off-grid communities. In *IECON 2012—38th annual conference on IEEE industrial electronics society* (pp. 5663–5668). Montreal, doi:10.1109/IECON.2012.6389060.

United Nations Foundation. (2012, June). Energy access practitioner network—towards achieving universal energy access by 2030.

Villalva, M. G., Gazoli, J. R., & Filho, E. R. (2009). Comprehensive approach to modeling and simulation of photovoltaic arrays. *IEEE Transactions on Power Electronics, 24*(5), 1198–1208.

http://www.springer.com/978-3-319-15963-8

Decentralized Solutions for Developing Economies
Addressing Energy Poverty Through Innovation
Groh, S.; van der Straeten, J.; Edlefsen Lasch, B.;
Gershenson, D.; Leal Filho, W.; Kammen, D. (Eds.)
2015, XXIV, 294 p. 84 illus., 25 illus. in color., Hardcover
ISBN: 978-3-319-15963-8